J. Earth Syst. Sci. (2021)130 106
https://doi.org/10.1007/s12040-021-01582-6

Comparison of the absorption characteristics of coloured dissolved organic matter between river and wave dominated distributaries of Godavari estuary, India

N V H K Chari[1,2,*], Ch Venkateswararao[1] and P Shyamala[1]

[1]*Department of Physical Chemistry, Nuclear Chemistry and Chemical Oceanography, School of Chemistry, Andhra University, Visakhapatnam 530 003, India.*
[2]*Centre for Marine Living Resources and Ecology, Ministry of Earth Sciences, Kochi 682 508, India.*
**Corresponding author. e-mail: harinaroju@rediffmail.com*

MS received 1 January 2020; revised 20 January 2021; accepted 24 January 2021

Absorption spectra of coloured dissolved organic matter (CDOM) and their derived parameters such as, absorption coefficient and spectral slopes are useful to study the molecular weight distribution of DOM. Here CDOM absorption characteristics were assessed in two distributaries [Gautami (GGE) and Vasishta (VGE)] of the Godavari estuary to examine the differences in molecular weight characterization of CDOM and its origin with reference to the geomorphological features during post southwest monsoon (PSM), late northeast monsoon (LNM) and early southwest monsoon (ESM) seasons. In VGE, absorption coefficient ($a_{CDOM}350$) exhibited significant negative correlation with total suspended matter (TSM) and salinity during PSM and LNM due to the local anthropogenic inputs. In GGE, the values of spectral slope $S_{275–295}$, and $S_{350–400}$ were low and high, respectively during PSM, indicating the presence of pronounced terrestrial derived organic matter. In VGE, $S_{350–400}$ showed increasing and decreasing trends from upstream to downstream in surface and bottom waters respectively during LNM, indicating that organic matter originated through *in-situ* microbiological processes. The spectral slope ratio, S_R ($S_{275–295}$/$S_{350–400}$) was higher in GGE during LNM (Avg ± SD = 1.19 ± 0.14) and ESM (1.47 ± 0.27), which suggests the lower molecular weight organic matter formation through microbiological and photodegradation processes. However, in VGE, the values of S_R during LNM (1.04 ± 0.11) and ESM (1.08 ± 0.17) were low, which indicates higher molecular weight organic matter formation due to biological production driven by local anthropogenic inputs or aquaculture effluents.

Keywords. Coloured dissolved organic matter; spectral slope; spectral slope ratio; Gautami Godavari; Vasishta Godavari.

Supplementary material pertaining to this article is available on the *Journal of Earth System Science* website (http://www.ias.ac.in/Journals/Journal_of_Earth_System_Science).

Published online: 27 May 2021

1. Introduction

Dissolved organic matter (DOM) is the dominant form of organic matter (OM) in the aquatic environments (Hansell and Carlson 2002). Estuaries receive DOM (Berman and Bronk 2003) through allochthonous (e.g., terrestrial OM from fresh water discharges from land, domestic sewage, and atmospheric deposition) and autochthonous (e.g., *in-situ* phytoplankton and bacteria production, and grazer input) sources (Bianchi 2006; Hedges and Keil 1999; Middelburg and Herman 2007). The fraction of DOM, which absorbs radiation in the UV-visible range, is referred to as coloured dissolved organic matter (CDOM). The quantity and quality (molecular weight distribution) of CDOM vary significantly in estuarine and coastal environments due to flocculation (Asmala *et al.* 2014), microbial uptake, bacterial degradation (Raymond and Bauer 2001; Kirchman *et al.* 2004) and photo transformation (Helms *et al.* 2008; Aarnos *et al.* 2012) processes. The coefficients and spectral slopes derived from absorption spectra are good indicators of concentration and molecular composition of CDOM. Absorption coefficients are used to quantify CDOM that contains specific organic compounds such as lignin phenol and their degradation products (Stedmon and Nelson 2015). The absorption spectrum in the UV range (200–400 nm) is often used to study CDOM because majority of aromatic compounds that constitute CDOM have their characteristic absorption maxima in this wavelength range (Peacock *et al.* 2013; Osburn *et al.* 2016; Fichot *et al.* 2016). Simple aromatic compounds that occur in aquatic environments mostly exhibit strong absorption below 350 nm but their absorption maxima increases and spectra broaden following their transformation through conjugation and substitution processes (Stedmon and Nelson 2015). There is only a small group of compounds of CDOM that exhibits smooth and featureless shape of the absorption spectrum at > 350 nm (Andrew *et al.* 2013; Boyle *et al.* 2009). Therefore the absorption coefficient ($a_{CDOM}350$), Spectral slopes ($S_{275-295}$ and $S_{350-400}$) and Spectral slope ratio (S_R, $S_{275-295}/S_{350-400}$) calculated based on absorption at wavelengths in the UV range provide information on concentration, origin (terrestrial or *in-situ* derived) and molecular weight distributions of CDOM in the estuarine and coastal environments. Lower value of $S_{275-295}$ is indicative of high terrestrial DOM and that of higher, the photochemical and microbiologically produced OM. Higher $S_{350-400}$ and S_R are indicative of the higher aromatic and lower molecular weight organic compounds and vice-versa in river and estuarine environments (Helms *et al.* 2008; Fichot and Benner 2012).

Estuaries are the transition zones between riverine and marine habitats and are geomorphologically dynamic and consist of many different habitat types (Meire *et al.* 2005). Absorbance spectra of CDOM increases exponentially with the decrease in wavelength (Twardowski *et al.* 2004). Studies on CDOM have been conducted in estuaries of different geomorphological types such as Chesapeake Bay (coastal plain, Tzortziou *et al.* 2001), San Franscisco Bay (tectonic, Fichot *et al.* 2016), South Atlantic bight (bar-built, Kowalczuk *et al.* 2010), Puget sound (fjord, Osburn *et al.* 2016), Pearl (river dominated, Chen *et al.* 2004), and Amazon river (tide dominated, Salisbury *et al.* 2011). Though studies on CDOM have been conducted in Indian estuarine systems [Mondovi-Zuari estuarine system (Menon *et al.* 2011), Godavari estuary (Chari *et al.* 2019) and Chilika lagoon (Sahay *et al.* 2019)], and in coastal waters of the Bay of Bengal (Pandi *et al.* 2017; Das *et al.* 2017) and the Arabian sea (Dias *et al.* 2017), no specific attempt has been made to understand CDOM characteristics in relation to estuarine geomorphological features and to natural and anthropogenic activities. Therefore, this study was conducted on estuarine systems of Gautami (river-dominated, GGE) and Vasishta (tide-dominated, VGE) distributaries of the Godavari river, which are surrounded by extensive mangroves and spaced sand ridges, respectively.

2. Materials and Methods

2.1 *Study area and field observations*

The Godavari is the largest peninsular river system in India and occupies a catchment area (3.1×10^5 km^2) of $\sim 9.5\%$ of the sub-continent. This river originates near Nasik in the Western Ghats mountain range and traverses eastward for ~ 1465 km before draining into the Bay of Bengal. Its basin receives rainfall of about 1000–1100 mm y^{-1} (Rao *et al.* 2015) with the highest ($\sim 84\%$) occurring during the southwest monsoon (June to September). Its annual discharge is ~ 105 km^3, which occurs through 25 tributaries. At Dowleswaram, it bifurcates into two main distributaries

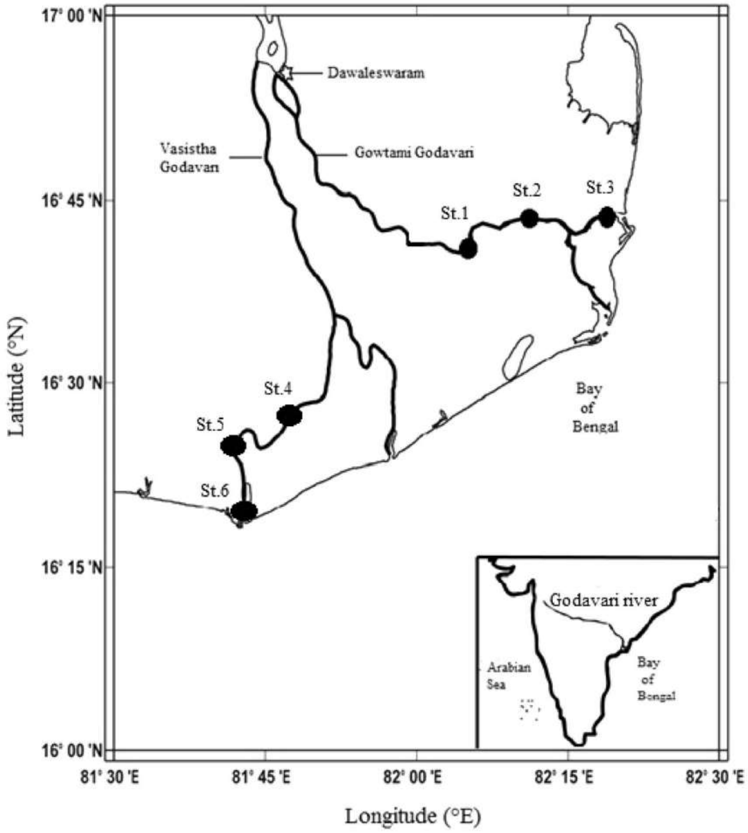

Figure 1. Station location map and sampling stations (●).

Table 1. *Summary of hydrochemical parameters in Vasishta Godavari.*

	Post-southwest monsoon			Late northeast monsoon			Early southwest monsoon		
	Min	Max	Avg ± SD	Min	Max	Avg ± SD	Min	Max	Avg ± SD
Salinity (‰)	0.30	22.99	10.50 ± 9.12	12.19	27.00	19.56 ± 6.76	4.12	34.45	19.56 ± 13.14
Temp (°C)	29.00	30.00	29.25 ± 0.42	27.00	29.50	28.17 ± 0.88	30.50	33.50	32.17 ± 1.21
DO (μM)	160	265	207 ± 45	200	265	243 ± 23	165	270	229 ± 38
Saturation (%)	69	103	85 ± 14	90	115	106 ± 8	77	152	110 ± 25
Chl *a* (mg m^{-3})	4.76	31.34	17.61 ± 10.11	1.27	5.51	3.07 ± 1.53	3.65	14.45	10.26 ± 4.16
TSM (mg dm^{-3})	6.2	16.94	10.31 ± 3.74	8.1	22.4	14.91 ± 6.78	5.76	29.9	16.01 ± 10.14

Min: minimum; Max: maximum; Avg: average; SD: standard deviation; Temp: temperature; DO: dissolved oxygen; μM: micro moles; Chl *a*: chlorophyll *a*; TSM: total suspended matter.

Vasishta Godavari and Gautami Godavari, which form the western and eastern parts of the Godavari estuarine system (figure 1). The significant geomorphological differences between these two estuaries include: (a) the GGE has an average width of ∼1200 m and surrounded by extensive mangrove swamps intermixed with thin beach ridges, whereas VGE is ∼900 m wide and surrounded by closely spaced ridge plains, and (b) the GGE discharges higher volume (∼67%) of fresh-water than by the VGE. In view of these differences GGE and VGE have been classified as river and wave dominated estuaries respectively, (Nageswara Rao *et al.* 2005) and significant variations in hydrochemical characteristics between these two systems have been found by Chari *et al.* (2020).

Seasonal observations of hydrochemical and CDOM absorption characteristics were carried out at three stations each in GGE and VGE covering the respective estuarine mixing zones (figure 1), Stations 1, 2 and 3 are located at Kotipalli, Yanam and Bhairavapalem in GGE, and those of 4, 5 and 6 are at Razole, Narsapur and Antarvedi in VGE. These stations represent Upper (UE), Middle (ME) and Lower Estuary (LE) mixing zones in the respective systems. The present study covered three seasons: post southwest monsoon (PSM, October 2016), late northeast monsoon (LNM, February 2017) and early southwest monsoon (ESM, June 2017).

2.2 *Sample collection and analyses*

Water samples for CDOM were collected in amber coloured glass bottles and immediately preserved in ice box (4°C) and filtered soon after reaching the laboratory, through 0.22 μ membrane filters of 25 mm diameter, under dim light. Absorption spectra were recorded between 200 and 800 nm at

Table 2. *Summary of hydrochemical parameters in Gautami Godavari.*

	Post-southwest monsoon			Late northeast monsoon			Early southwest monsoon		
	Min	Max	Avg ± SD	Min	Max	Avg ± SD	Min	Max	Avg ± SD
Salinity (‰)	0.16	17.33	7.61 ± 7.11	10.79	29.71	21.83 ± 8.30	1.50	29.77	19.25 ± 13.44
Temp (°C)	29.00	31.00	30.00 ± 0.63	29.00	30.00	29.46 ± 0.41	29.50	30.50	30.33 ± 0.41
DO (μM)	185	311	242 ± 51	186	233	215 ± 19	218	270	248 ± 17
Saturation (%)	78	124	99 ± 17	78	109	96 ± 10	98	125	110 ± 12
Chl *a* (mg m^{-3})	4.66	26.34	14.98 ± 9.10	2.83	6.72	4.36 ± 1.31	3.25	11.36	7.34 ± 2.97
TSM (mg dm^{-3})	2.28	28.88	11.11 ± 9.70	7.89	34.16	19.34 ± 9.96	9.2	37.60	26.21 ± 12.73

Min: Minimum; Max: Maximum; Avg: Average; SD: Standard Deviation; Temp: Temperature; DO: Dissolved Oxygen; μM: Micro Moles; Chl *a*: Chlorophyll *a*; TSM: Total Suspended Matter.

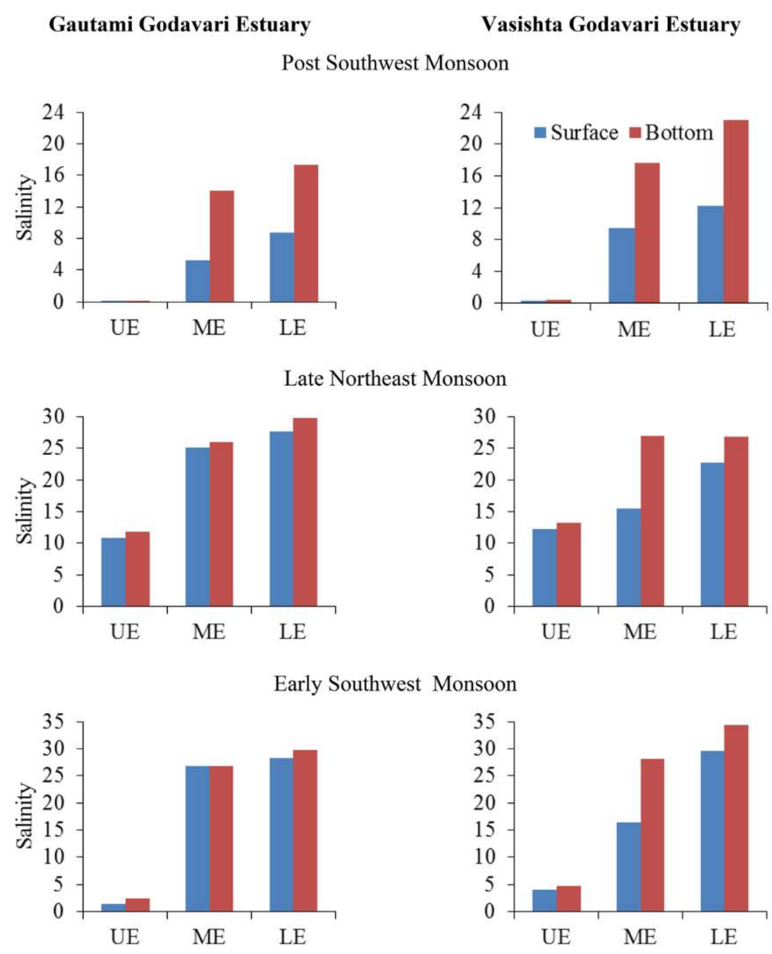

Figure 2. Seasonal distribution of salinity in the Gautami and Vasishta Godavari estuaries during post-southwest monsoon (PSM), late northeast monsoon (LNM) and early southwest monsoon (ESM).

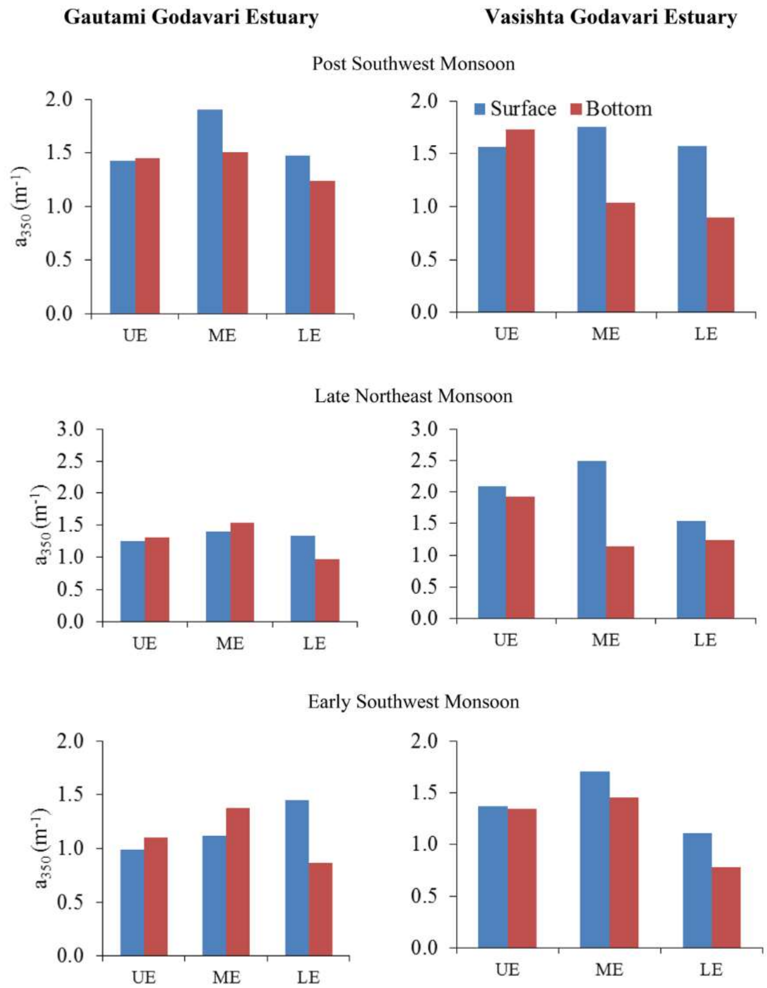

Figure 3. Seasonal distribution of $a_{CDOM}350$ (m^{-1}) in the Gautami and Vasishta Godavari estuaries.

an interval of 1 nm using Shimadzu UV-visible 1800 double-beam spectrophotometer and 10 cm path length quartz cuvettes. Milli-Q water was used as a reference. Null point correction was applied to all samples at 700 nm for uniformity (Shank *et al.* 2009). Absorption coefficients were calculated using the equation

$$a = 2.303A/l,$$

where a is the absorption coefficient (m^{-1}), A is the absorbance and l is the path length (m).

Spectral slope (S) was calculated for the regions 275–295 and 350–400 nm using an exponential regression model between the absorption coefficient and wavelength. $S_{330–440}$ was suggested to be used in the Godavari estuary to overcome the peaks in the wavelength range (260–280 nm) of humic or protein like organic compounds (Sarma *et al.* 2018). However, our comparative experiments (see supplementary data) revealed similar trends between values of $S_{330–440}$ and $S_{350–400}$ and hence we preferred to use only the latter.

$$a(\lambda) = a(\lambda_0)e^{-s(\lambda-\lambda_0)},$$

where $a(\lambda)$ is the absorption coefficient at wavelength λ, $a(\lambda_0)$ the absorption coefficient at the reference wavelength λ_0 and S is the spectral slope. The spectral slope ratio (S_R) was then calculated as the ratio of $S_{275–295}$ to $S_{350–400}$.

3. Results and discussion

3.1 *Hydrochemical parameters*

The Summary of hydrochemical parameters of GGE and VGE are listed in tables 1 and 2 respectively. Salinity increased from UE to LE in all seasons in both the estuaries (figure 2). The differences in salinity between surface and bottom waters (~5 to

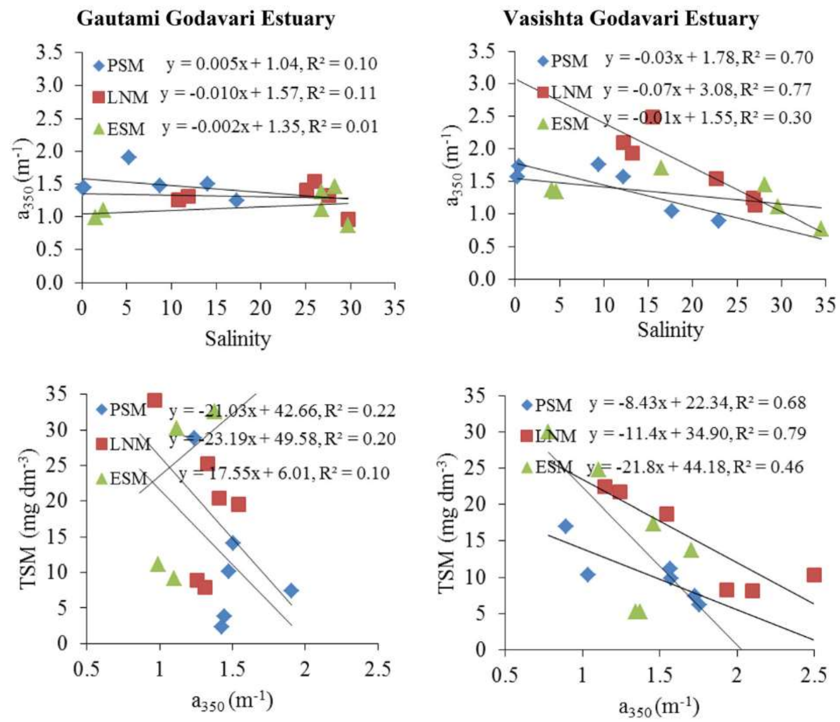

Figure 4. Relation between the a_{350} (m^{-1}) with salinity and TSM in Gautami and Vasishta Godavari estuary.

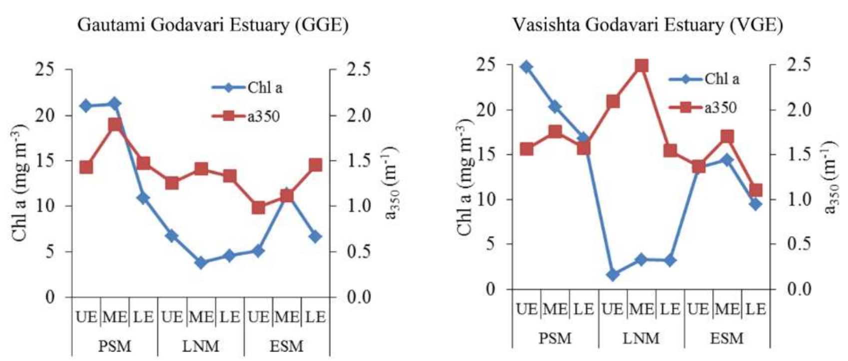

Figure 5. Variation of Chl *a* and a_{350} (m^{-1}) in the surface waters of Gautami and Vasishta Godavari estuary during the three seasons (PSM: post-southwest monsoon; LNM: late northeast monsoon; ESM: early southwest monsoon).

8 m) were higher in VGE than in GGE, particularly during LNM and ESM. The wave-dominated nature of VGE facilitates observed vertical differences in salinity. This finding is consistent with the vertical stratification in VGE, which is attributed to strong saline water intrusion (Nageswara Rao *et al.* 2005). During LNM, dissolved oxygen (DO) exhibited high concentrations in VGE than in GGE (tables 1 and 2). This is due to the higher primary production in the VGE (Chari *et al.* 2020) and is consistent with DO super saturation (Avg $\pm$ SD $= 106 \pm 8\%$). On the other hand, net heterotrophy conditions prevailed in GGE because of the bacterial degradation of organic matter, which is in agreement with the observations of Sarma *et al.* (2009). The total suspended matter (TSM) showed large variability and its concentration was high in GGE in all seasons, due to the dominance of discharges from land and local (through mangroves and anthropogenic) inputs. Nutrients ($NO_3^- - N$, $PO_4{}^{3-}$–P and $SiO_4{}^{4-}$–Si) exhibited conservative behaviour in GGE, but non-conservative behaviour in VGE, due to dominance of biological processes in the latter (Chari *et al.* 2020).

3.2 *Relations of $a_{CDOM}350$ with hydrochemical parameters*

The coefficient $a_{CDOM}350$ (m^{-1}) ranged from 0.86 to 1.32 and from 0.78 to 2.49 in GGE and VGE, respectively. These values are within the range reported for GGE (Chari *et al.* 2019) and adjacent

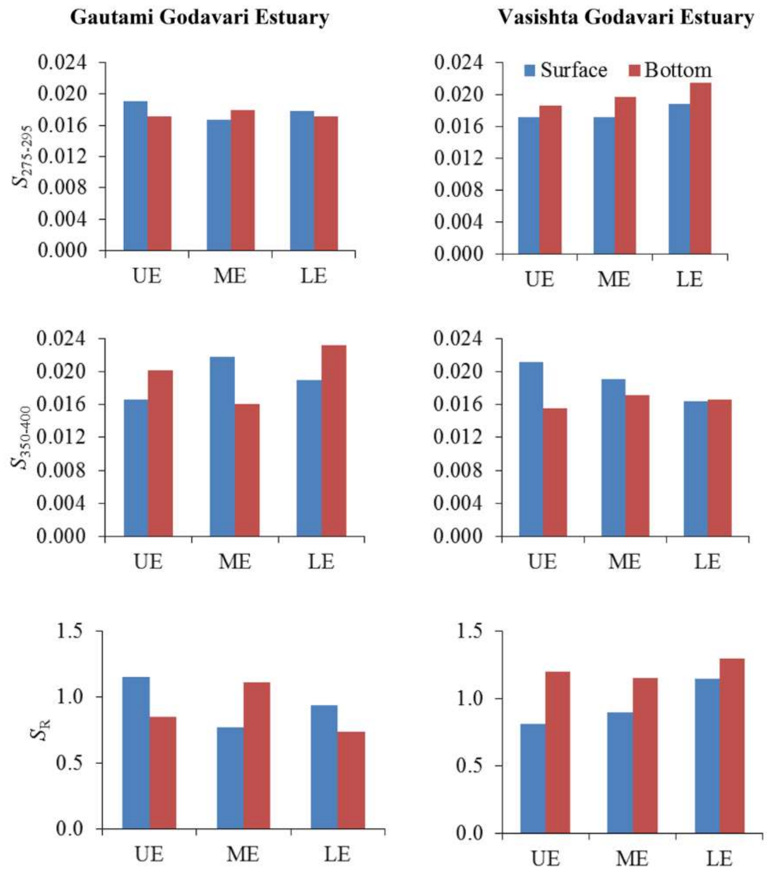

Figure 6. Variation of $S_{275–295}$, $S_{350–400}$ and S_R during PSM season in GGE (Gautami Godavari Estuary) and VGE (Vasishta Godavari Estuary).

coastal waters of the Bay of Bengal (Chiranjeevulu *et al.* 2014). In GGE, $a_{CDOM}350$ did not show significant vertical variation in all seasons (figure 3), which indicates that the water column was mixed. Since this study was conducted during the lean to nil discharge periods, intrusion of saline water might be significant. This observation is in agreement with that of Sridevi *et al.* (2015) wherein saline water intrudes to about ∼36 km upstream from the mouth of GGE during dry periods. However, in VGE, $a_{CDOM}350$ was higher at surface than in bottom waters in all seasons except in the UE zone during PSM. This indicates partially mixed water conditions during all the three sampling periods in this study. The $a_{CDOM}350$ showed significant negative correlations with salinity ($n = 6$, $r = 0.84$, 0.87, $p = 0.04$, 0.02) and TSM ($n = 6$, $r = 0.82$, 0.89, $p = 0.04$, 0.02) during PSM and LNM in VGE, but in GGE the same were not statistically significant (figure 4). Since, the fresh water input was minimal during the observation periods *in-situ* OM production driven by anthropogenic nutrients inputs might be the source of CDOM in VGE. Moreover, during the LNM, increase in $a_{CDOM}350$ with decrease of Chl a in surface waters was prominent in VGE than that in GGE (figure 5). This augments the organic matter degradation as being the source of CDOM (Zhang *et al.* 2009) in VGE during LNM. However, in GGE absence of these correlations and low $a_{CDOM}350$ during LNM indicates that the modifications of CDOM (bacterial consumption or removal by adsorption) might be taking place through biogeochemical interactions. This observed trend is in agreement with the observation that heterotrophy conditions prevail in GGE during nil discharge periods (Sarma *et al.* 2009).

3.3 *Seasonal variations in $S_{275–295}$, $S_{350–400}$ and S_R*

Lower $S_{275–295}$ (nm^{-1}) of 0.0176 ± 0.0008 in GGE than in VGE (0.0188 ± 0.0016) in PSM indicates significantly higher terrestrial organic matter in the former region. On the other hand, it was higher in bottom (than in surface) waters and its increasing trend from UE to LE (figure 6) reveals its association with the intruding saline water in the VGE. In contrast, $S_{350–400}$ was found to be higher in the GGE (0.0195 ± 0.0028) than that in

VGE (0.0176 ± 0.0021) and the spectral slope at the shorter wavelength ($S_{275-295}$) was less than the longer wavelength range ($S_{350-400}$) indicating that the terrestrial derived organic matter (Helms *et al.* 2008) was more predominant in GGE. In fact, S_R, which was low in GGE (0.92 ± 0.17) than in VGE (1.08 ± 0.18) indicated the presence of high molecular weight terrestrial OM in the entire GGE supplied by fresh water discharges in southwest monsoon. In VGE, $S_{350-400}$ and S_R showed decreasing and increasing trends, respectively, from UE to LE in surface waters (figure 6), which can be attributed to lower molecular weight organic matter supply through partial mixing with seawater.

In LNM, $S_{275-295}$ did not show spatial or vertical variations of significance in both the regions. Its higher values found in GGE in LNM (0.0189 ± 0.0008) than in PSM (0.0176 ± 0.0008) indicate the significance of *in-situ* produced OM during nil discharge periods. The $S_{350-400}$ was lower in GGE (0.0160 ± 0.0012) during LNM than in PSM (0.0195 ± 0.0022) and gradually decreased from UE to LE in surface waters (figure 7). This is attributed to OM derived from *in-situ* biological activity at surface. This is corroborated with the earlier reports of phytoplankton blooms occurrence with the reduction in fresh water discharge in GGE (Sarma *et al.* 2009). Similar results were observed in other estuarine and coastal environments: with the reduction in terrestrial fresh water discharge humic-like organic matter is produced from the *in-situ* microbial process (Battin *et al.* 2008; Aufdenkampe *et al.* 2011). However, in VGE, $S_{350-400}$ was higher in LNM (0.0184 ± 0.0017) than in PSM (0.0176 ± 0.0021) and increasing and decreasing trends were observed from UE to LE in the surface and bottom waters respectively (figure 7). This is attributed to the *in-situ* produced OM associated with increase in primary production from UE to LE in surface waters, whereas in the bottom, intrusion of the saline water with low OM might have caused the reverse trend. The S_R showed inverse trends to that of $S_{350-400}$ and was lower in VGE (1.04 ± 0.11) than in GGE (1.19 ± 0.14), which suggests that the higher molecular weight organic matter (low S_R) was formed by *in-situ* microbiological process (Helms *et al.* 2008) in the former region. However, in GGE, in addition to the *in-situ* phytoplankton production, bacterial respiration is

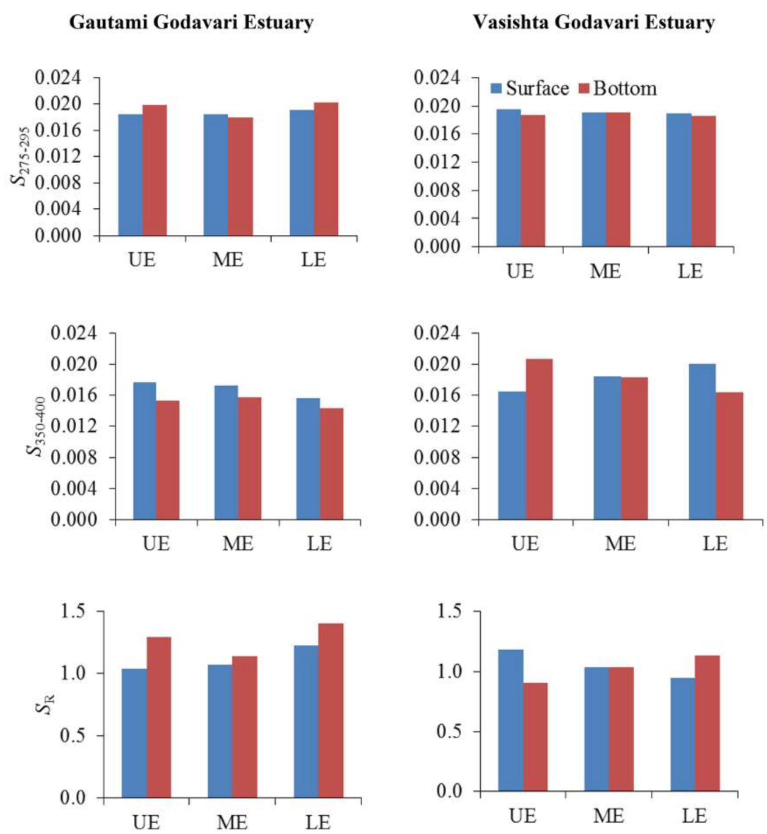

Figure 7. Variation of $S_{275-295}$, $S_{350-400}$ and S_R during LNM season in GGE (Gautami Godavari Estuary) and VGE (Vasishta Godavari Estuary).

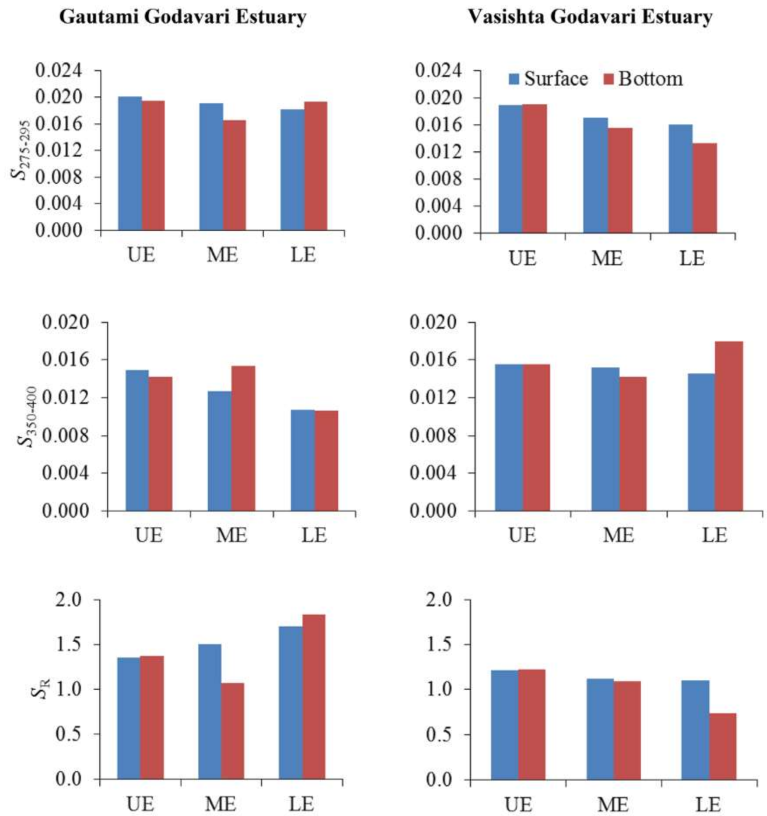

Figure 8. Variation of $S_{275-295}$, $S_{350-400}$ and S_R during ESM season in GGE (Gautami Godavari Estuary) and VGE (Vasishta Godavari Estuary).

found to be significantly high (Sarma *et al.* 2009) and hence low molecular weight OM (high S_R) seems to occur.

There were no significant variations in $S_{275-295}$ from LNM to ESM and from UE to LE in GGE. But in VGE, $S_{275-295}$ was lower in ESM (0.0166 ± 0.0022) than in other seasons and its gradual decreasing trend from UE to LE in both surface and bottom waters (figure 8) was observed. This indicates the presence of refractory organic compounds in the ME and LE, which might have been due to effluents discharged by aquaculture ponds (Sadeghi-Nassaj *et al.* 2018) during this season. $S_{350-400}$ was found to be low in GGE (0.0131 ± 0.0021) during ESM than in other seasons and the gradual decrease of $S_{350-400}$ in surface waters of GGE from UE to LE occurred (figure 8). This is due to the degradation of organic matter by microbial processes (Hansen *et al.* 2016), which varied spatially within the estuary. But in VGE $S_{350-400}$ (0.0151 ± 0.0004) was consistently higher than in GGE, indicating that the fulvic acid-like organic compounds (Mostofa *et al.* 2005) might have been released from adjacent aquaculture ponds. The $S_{275-295} > S_{350-400}$ indicates that low molecular weight marine-derived dissolved organic matter (Chen *et al.* 2011) was more pronounced and significantly high in GGE. However, in VGE (1.08 ± 0.18) low values of S_R than in GGE (1.47 ± 0.27) suggest that higher molecular weight OM was predominant in the former region due to discharges from aquaculture ponds.

Acknowledgements

This work was supported by the Department of Science and Technology, Science and Engineering Research Board to N V H K Chari under Grant No. SR/FTP/ES-56/2013. The authors thank the Prof Nittala S Sarma (Emeritus Scientist, CSIR) for the technical support and for providing the instrumental facilities. The authors are highly thankful to the anonymous reviewers for their critical comments and suggestions for improvement of the manuscript.

Author statement

N V H K Chari: Study plan; sampling; analysis, interpretation of results and drafting the manuscript. Ch Venkateswararao: Sampling, analysis

and presentation of results and modifications in the manuscript. P Shyamala: Procedural permissions-facilities, suggestions and developing the manuscript.

References

Aarnos H, Ylöstalo P and Vähätalo A V 2012 Seasonal phototransformation of dissolved organic matter to ammonium, dissolved inorganic carbon, and labile substrates supporting bacterial biomass across the Baltic Sea; *J. Geophys. Res.* **117** G01004.

Andrew A A, Del Vecchio R, Subramaniam A and Blough N V 2013 Chromophoric dissolved organic matter (CDOM) in the Equatorial Atlantic Ocean: Optical properties and their relation to CDOM structure and source; *Mar. Chem.* **148** 33–43.

Asmala E, Bowers D G, Auti R, Kaartokallo H and Thomas D N 2014 Qualitative changes of riverine dissolved organic matter at low salinities due to flocculation; *JGR Biogeosci.* **119** 1919–1933.

Aufdenkampe A K, Mayorga E, Raymond P A, Melack J M, Doney S C, Alin S R, Aalto R E and Yoo K 2011 Riverine coupling of biogeochemical cycles between land, oceans and atmosphere; *Front. Ecol. Environ.* **9** 53–60.

Battin T J, Kaplan L A, Findlay S, Hopkinson C S, Marti E, Packman A I, Newbold J C and Sabater F 2008 Biophysical controls on organic carbon fluxes in fluvial networks; *Nat. Geosci.* **1** 95–100.

Berman T and Bronk D 2003 Dissolved organic nitrogen: A dynamic participant in aquatic ecosystems; *Aqua. Microb. Ecol.* **31(3)** 279–305.

Bianchi T S 2006 *Biogeochemistry of Estuaries*; Oxford Univ. Press, Oxford, UK.

Boyle E S, Guerriero N, Thiallet A, Del Vecchio R and Blough N V 2009 Optical properties of humic substances and CDOM: Relation to structure; *Environ. Sci. Technol.* **43** 2262–2268.

Chari N V H K, Sudarsana Rao P, Vishnu Vardhan K and Charan Kumar B 2019 Structural variation of coloured dissolved organic matter during summer and winter seasons in a tropical estuary: A case study; *Mar. Pol. Bul.* **149** 110563.

Chari N V H K, Venkateswararao Ch, Muralikrishna R and Sivakrishna K 2020 Variation of hydrochemical parameters with reference to geomorphological features in Godavari estuary, India; *Ind. J. Mar. Sci.* **49** 24–33.

Chen H, Zheng B, Song J and Qin Y 2011 Correlation between molecular absorption spectral slope ratios and fluorescence humification indices in characterizing CDOM; *Aquat. Sci.* **73** 103–112.

Chen Z, Yan Li and Jianming P 2004 Distributions of colored dissolved organic matter and dissolved organic carbon in the Pearl River Estuary, China; *Cont. Shelf. Res.* **24** 1845–1856.

Chiranjeevulu G, Narasimhamurthy K, Sarma S N, Kiran R, Chari K H V N, Sudarsana Rao P, Venkatesh P, Annapurna C and Nageswara Rao K 2014 Colored dissolved organic matter signature and phytoplankton response in a coastal ecosystem during mesoscale cyclonic (cold core) eddy; *Mar. Environ. Res.* **98** 49–59.

Das S, Hazra S, Giri S, Das I, Chanda A, Akhand A and Maity S 2017 Light absorption characteristics of chromophoric dissolved organic matter (CDOM) in the coastal waters of northern Bay of Bengal during winter season; *Ind. J. Geo-Mar. Sci.* **46** 884–892.

Dias A B, Suresh T, Sahay A and Chauhan P 2017 Contrasting characteristics of colored dissolved organic matter of the coastal and estuarine waters of Goa during summer; *Ind. J. Geo-Mar. Sci.* **46** 860–870.

Fichot C G and Benner R 2012 The spectral slope coefficient of chromophoric dissolved organic matter ($S_{275–295}$) as a tracer of terrigenous dissolved organic carbon in river-influenced ocean margins; *Limnol. Oceanogr.* **57** 1453–1466.

Fichot G C, Benner R, Kaiser K, Shen Y, Amon R M W, Ogawa H and Jung L-C 2016 Predicting dissolved lignin phenol concentrations in the coastal ocean from chromophoric dissolved organic matter (CDOM) absorption coefficients; *Front. Mar. Sci.* **3** 7.

Hansen A M, Kraus T E C, Pellerin B A, Fleck J A, Downing B D and Bergamaschi B A 2016 Optical properties of dissolved organic matter (DOM): Effects of biological and photolytic degradation; *Limnol. Oceanogr.* **61** 1015–1032.

Hansell D A and Carlson C A 2002 *Biogeochemistry of marine dissolved organic matter*; Academic Press USA, 774p.

Hedges J I and Keil G R 1999 Organic geochemical perspectives on estuarine processes: Sorption reactions and consequences; *Mar. Chem.* **65** 55–65.

Helms J R, Stubbins A, Ritchie J D, Minor E C, Kieber D J and Mopper K 2008 Absorption spectral slopes and slope ratios as indicators of molecular weight, source, and photo bleaching of chromophoric dissolved organic matter; *Limnol. Oceanogr.* **53** 955–969.

Kirchman D L, Dittel A I, Findlay S E G and Fischer D 2004 Changes in bacterial activity and community structure in response to dissolved organic matter in the Hudson River, New York; *Aqua. Micro. Eco. (AME)* **35** 243–257.

Kowalczuk P, Cooper W J, Durako M J, Kahn A E, Gonsior M and Young H 2010 Characterization of dissolved organic matter fluorescence in the South Atlantic Bight with use of PARAFAC model: Relationships between fluorescence and its components, absorption coefficients and organic carbon concentrations; *Mar. Chem.* **118** 22–36.

Meire P, Ysebaert T, Damme Van S, Van den bergh E, Maris T and Struyf E 2005 The Scheldt estuary: A description of changing ecosystem; *Hydrobiologia* **540** 1–11.

Menon H B, Sangekar P N, Lotliker A A and Vethamony P 2011 Dynamics of chromophoric dissolved organic matter in Mandovi and Zuari estuaries – A study through *in-situ* and satellite data; *ISPRS J. Photogramm. Remote Sens.* **66** 545–552.

Middleburg J J and Herman P M J 2007 Organic matter processing in tidal estuaries *Mar. Chem.* **10** 127–147.

Mostofa K M G, Honda Y and Sakugawa H 2005 Dynamics and optical nature of fluorescent dissolved organic matter in river waters in Hiroshima Prefecture, Japan; *Geochem. J.* **39** 257–271.

Nageswara Rao K, Sadakata N, Hema Malini B and Takayasu K 2005 Sedimentation processes and asymmetric development of the Godavari deltas, India; SEPM (*Society for Sedimentary Geology) Spec. Publ.* **83** 435–451.

Osburn C L, Boyd T J, Montgomery M S, Blanchi T S, Coffin R B and Paerl H W 2016 Optical proxies for terrestrial dissolved organic matter in estuaries and coastal waters; *Front. Mar. Sci.* **2** 127, https://doi.org/10.3389/fmars.2015.00127.

Pandi S R, Gundala C, Rayaprolu K, Naroju V H, Rallabhandi M, Balivada S, Lotliker A A and Sarma N S 2017 Contrasting bio-optical characterstics of coastal water prior to and in the aftermath of a tropical super cyclone; *Int. J. Remote. Sens.* **38** 3519–3530.

Peacock M, Burden A, Cooper M, Dunn C, Evans C D, Fenner N, Freeman C, Gough R, Hughes D and Hughes S 2013 Quantifying dissolved organic carbon concentrations in upland catchments using phenolic proxy measurements; *J. Hydrol.* **477** 251–260.

Rao K N, Saito Y, Nagakumar K C V, Demudu G, Rajawat A S, Kubo S and Zhen L 2015 Palaeogeography and evolution of the Godavari delta, east coast of India during the Holocene: An example of wave-dominated and fan-delta settings; *Palaeogeogr. Palaeoclimatol. Palaeoecol.* **440** 213–233.

Raymond P A and Bauer J E 2001 DOC cycling in a temperate estuary: A mass balance approach using natural ^{14}C and^{13}C isotopes; *Limnol. Ocenogr.* **46** 655–667.

Sadeghi-Nassaj S M, Catalá T S, Álvarez P A and Reche I 2018 Sea cucumbers reduce chromophoric dissolved organic matter in aquaculture tanks; *Peer J.* **6** e4344.

Sarma N S, Pandi S R, Chari N V H K, Chiranjeevulu G, Kiran R, Krishna K S, Rao D B, Venkatesh P, Kumar B C and Raman A 2018 Spectral modelling of estuarine coloured dissolved organic matter, *Curr. Sci.* **114** 1762–1767.

Sahay A, Gupta A, Motwani G, Raman M, Ali S M, Shah M, Chander S, Muduli P R and Samal R N 2019 Distribution of coloured dissolved and detrital organic matter in optically complex waters of Chilika lagoon, Odisha, India, using hyperspectral data of AVIRIS-NG; *Curr. Sci.* **116** 1166–1171.

Salisbury J, Vandemark D, Campbell J, Hunt C, Wisser D, Reul N and Chapron B 2011 Spatial and temporal coherence between Amazon River discharge, salinity, and light absorption by colored organic carbon in western tropical Atlantic surface waters; *J. Geophys. Res.* **116** C00H02.

Shank C G, Nelson K and Montagna K 2009 Importance of CDOM distribution and photo reactivity in a shallow Texas Estuary; *Estur. Coasts.* **32** 661–677.

Sridevi B, Sarma V V S S, Murty T V R, Sadhuram Y, Reddy N P C, Vijaykumar K, Raju N S N, Jawahar Kumar C H, Raju Y S N, Luis R, Kumar M D and Prasad K V S R 2015 Variability in stratification and flushing times of the Gautami–Godavari estuary, India; *J. Earth Syst. Sci.* **124** 993–1003.

Stedmon C A and Nelson N B 2015 The optical properties of DOM in the ocean; In: *Biogeochemistry of Marine Dissolved Organic Matter*, 2nd edn (eds) Hansell C D and Carlson E, San Diego CA, USA, Academic Press, pp. 481–508.

Sarma V V S S, Gupta S N M, Babu P V R, Acharayya T, Harikrishnachari N, Vishnuvardhan K, Rao N S, Reddy N P C, Sarma V V, Sadhuram Y, Murthy T V R and Kumar M D 2009 Influence of river discharge on plankton metabolic rates in the tropical monsoon driven Godavari estuary, India; *Estur. Coast. Shelf. Sci.* **85** 515–524.

Twardowski M S, Boss E, Sullivan J M and Donaghay P L 2004 Modeling the spectral shape of absorption by chromophoric dissolved organic matter; *Mar. Chem.* **89** 69–88.

Tzortziou M, Neale P J, Osburn C L, Megonigal J P, Maie N, JaffÉ G U, Hughes C, Henry G and Upstill-Goddard R C 2001 Non-conservative mixing behavior of colored dissolved organic matter in a humic-rich, turbid estuary; *Geophys. Res. Lett.* **28** 3309–3312.

Zhang Y L, Van Dijk M A, Liu M L, Zhu G W and Qin B Q 2009 The contribution of phytoplankton degradation to chromophoric dissolved organic matter (CDOM) in eutrophic shallow lakes: Field and experimental evidence; *Water Res.* **43** 4685–4697.

Corresponding editor: Maripi Dileep